Synthesis and Characterization of the Manganese Borate α-MnB_2O_4

Stephanie C. Neumair[a], Lukas Perfler[b], and Hubert Huppertz[a]

[a] Institut für Allgemeine, Anorganische und Theoretische Chemie, Leopold-Franzens-Universität Innsbruck, Innrain 52a, 6020 Innsbruck, Austria
[b] Institut für Mineralogie und Petrographie, Leopold-Franzens-Universität Innsbruck, Innrain 52f, 6020 Innsbruck, Austria

Reprint requests to H. Huppertz. E-mail: Hubert.Huppertz@uibk.ac.at

Z. Naturforsch. **2011**, *66b,* 882 – 888; received July 26, 2011

The high-pressure manganese borate α-MnB_2O_4 was synthesized under high-pressure/high-temperature conditions of 6.5 GPa and 1100 °C in a modified Walker-type multianvil apparatus. The monoclinic compound is isotypic to α-FeB_2O_4, $CaAl_2O_4$-II, $CaGa_2O_4$, and β-$SrGa_2O_4$ crystallizing with eight formula units in the space group $P2_1/c$ ($Z = 8$) with the lattice parameters $a = 712.1(2)$, $b = 747.1(2)$, $c = 878.8(2)$ pm, $\beta = 94.1(1)°$, $V = 0.466(1)$ nm^3, $R_1 = 0.0326$, and $wR_2 = 0.0652$ (all data). The compound is built up from layers of "sechser" rings of corner-sharing BO_4 tetrahedra that are interconnected to a three-dimensional network. The manganese ions are coordinated by seven oxygen atoms and situated in channels along the *a* axis.

Key words: High Pressure, Borate, Crystal Structure

Introduction

The application of high pressure in the synthesis of borates allows new insights into the structural and synthetic possibilities of borate chemistry [1]. *Via* high-pressure synthesis, new polymorphs (*e. g.* δ-BiB_3O_6 [2]), and compounds with new compositions (*e. g.* β/HP-MB_2O_4 (M = Fe, Co, Ni) [3 – 5], $M_6B_{22}O_{39} \cdot H_2O$ (M = Fe, Co) [6]) could be obtained. In the ternary system Mn-B-O, our high-pressure investigations led to the first manganese high-pressure borate β-MnB_4O_7 [7], which consists exclusively of BO_4 tetrahedra and is isotypic to β-MB_4O_7 (M = Fe, Co, Ni, Cu, Zn) [7 – 9].

Under ambient pressure, ternary manganese borates show a variety of compositions. One example is α-MnB_4O_7 [10], which exhibits BO_4 tetrahedra and planar BO_3 groups. In addition, there are the manganese borates and oxoborates $Mn_3(BO_3)_2$ [11, 12], $Mn_3(BO_3)O_2$ [13], and Mn_2OBO_3 [14] with BO_3 units only. In accordance with the pressure-coordination rule, the application of high pressure to borates with BO_3 units could lead to new manganese borates with higher contents of BO_4 tetrahedra, as was proven with the synthesis of β-MnB_4O_7 [7]. Further systematic high-pressure investigations into the ternary manganese borates led to the α-MnB_2O_4 presented here, which also consists exclusively of BO_4 tetrahedra. It is isotypic to α-FeB_2O_4 [15] and $CaAl_2O_4$-II [16, 17], as well as to the normal-pressure phases $CaGa_2O_4$ [18] and β-$SrGa_2O_4$ [19]. In this paper, the synthesis, crystal structure and properties of α-MnB_2O_4 are discussed and compared to the isotypic phase α-FeB_2O_4.

Experimental Section

Synthesis

α-MnB_2O_4 was synthesized in a modified Walker-type multianvil apparatus under high-pressure/high-temperature conditions of 6.5 GPa and 1100 °C.

To synthesize α-MnB_2O_4, a non-stoichiometric mixture of MnO_2 and B_2O_3 (Strem Chemicals, Newburyport, USA, 99.9 %) in a molar ratio of 2 : 1 was finely ground and filled into a boron nitride crucible (Henze BNP GmbH, HeBoSint® S100, Kempten, Germany). The crucible was placed into an 18/11-assembly and compressed by eight tungsten carbide cubes (TSM-10, Ceratizit, Reutte, Austria). To apply the pressure, a 1000 t multianvil press with a Walker-type module (both devices from the company Voggenreiter, Mainleus, Germany) was used. The assembly and its preparation are described in detail in refs. [20 – 24].

In order to synthesize α-MnB_2O_4, the mixture of the starting materials was compressed to 6.5 GPa within 3 h and kept at this pressure. During the heating period, the temperature was increased to 1100 °C in 30 min, kept there for 10 min, and lowered to 430 °C within 15 min. Afterwards, the sample was cooled to room temperature by switching off

0932–0776 / 11 / 0900–0882 $ 06.00 © 2011 Verlag der Zeitschrift für Naturforschung, Tübingen · http://znaturforsch.com

Table 1. Crystal data and structure refinement of α-MnB_2O_4 (standard deviations in parentheses).

Empirical formula	α-MnB_2O_4
Molar mass, g mol^{-1}	140.56
Crystal system	monoclinic
Space group	$P2_1/c$
Powder diffractometer	Stoe Stadi P
Radiation; wavelength, pm	Mo$K_{\alpha1}$; 70.93
a, pm	711.8(2)
b, pm	747.1(2)
c, pm	878.1(2)
β, deg	94.1(1)
V, nm^3	0.4658(2)
Single-crystal diffractometer	Enraf-Nonius Kappa CCD
Radiation; λ, pm	MoK_α; 71.073
Single-crystal data	
a, pm	712.1(2)
b, pm	747.1(2)
c, pm	878.8(2)
β, deg	94.1(1)
V, nm^3	0.4663(2)
Formula units per cell Z	8
Calculated density, g cm^{-3}	4.00
Crystal size, mm^3	$0.05 \times 0.10 \times 0.11$
Temperature, K	293(2)
Absorption coefficient, mm^{-1}	5.4
Absorption correction	multi-scan [26]
F(000), e	536
θ range, deg	2.9–37.8
Range in hkl	$-11 \le h \le 12$, $-12 \le k \le 12$, $-13 \le l \le 15$
Total no. of reflections	7530
Independent reflections / R_{int} / R_σ	2489 / 0.0362 / 0.0361
Reflections with $I \ge 2\sigma(I)$	2272
Data / ref. parameters	2489 / 128
Goodness-of-fit on F_i^2	1.076
Final $R1$ / $wR2$ [$I \ge 2\sigma(I)$]	0.0279 / 0.0638
$R1$ / $wR2$ (all data)	0.0326 / 0.0652
Largest diff. peak / hole, e Å^{-3}	0.98 / −0.86

the heating, followed by a decompression period of 9 h. The recovered pressure medium was broken apart and the sample separated from the surrounding boron nitride crucible. The compound α-MnB_2O_4 was found in the form of brownish air-resistant crystals.

All efforts to get this compound from a stoichiometric mixture of the educts did not yield any α-MnB_2O_4, but it can also be synthesized from a non-stoichiometric mixture of $KMnO_4$ and B_2O_3 (6.5 GPa / 880 °C). This reaction leads, due to the additional potassium, to even more side products.

The manganese cations were reduced to the oxidation state 2+ during the synthesis. Such a reduction of the metal ions is often observed in the multianvil high-pressure assembly, and is described in ref. [7].

Crystal structure analysis

The powder diffraction pattern was obtained in transmission geometry, using a Stoe Stadi P powder diffractometer with Ge(111)-monochromatized Mo$K_{\alpha1}$ (λ = 70.93 pm) radiation. The diffraction pattern showed reflections of α-MnB_2O_4, of Jimboite ($Mn_3B_2O_6$), and those of at least one additional by-product of the synthesis. The experimental powder pattern tallies well with the theoretical pattern simulated from single-crystal data. On the basis of a monoclinic unit cell, the diffraction pattern was indexed with the program ITO [25]. The lattice parameters (Table 1) were calculated from least-squares fits of the powder data, which confirmed the lattice parameters, received from the single-crystal X-ray diffraction analysis (Table 1).

Table 2. Atomic coordinates (Wyckoff position 4*e* for all atoms) and equivalent isotropic displacement parameters U_{eq} (Å^2) of α-MnB_2O_4 (space group: $P2_1/c$) with standard deviations in parentheses. U_{eq} is defined as one third of the trace of the orthogonalized U_{ij} tensor.

Atom	x	y	z	U_{eq}
Mn1	0.99920(3)	0.21473(3)	0.12491(2)	0.00927(6)
Mn2	0.47006(3)	0.25663(3)	0.14327(2)	0.00843(6)
B1	0.6983(2)	0.1011(2)	0.8802(2)	0.0061(2)
B2	0.6881(2)	0.9023(2)	0.1162(2)	0.0058(2)
B3	0.2056(2)	0.4362(2)	0.8681(2)	0.0057(2)
B4	0.8175(2)	0.4324(2)	0.8621(2)	0.0059(2)
O1	0.2223(2)	0.2482(2)	0.3058(2)	0.0067(2)
O2	0.2309(2)	0.0591(2)	0.0318(2)	0.0064(2)
O3	0.5109(2)	0.1577(2)	0.9213(1)	0.0066(2)
O4	0.0097(2)	0.0045(2)	0.3273(2)	0.0073(2)
O5	0.8322(3)	0.2484(2)	0.9188(2)	0.0068(2)
O6	0.6768(2)	0.4419(2)	0.2160(2)	0.0068(2)
O7	0.7020(2)	0.0622(2)	0.2141(2)	0.0070(2)
O8	0.2596(2)	0.4400(2)	0.0312(2)	0.0072(2)

To perform the single-crystal structure analysis, small irregularly shaped crystals of α-MnB_2O_4 were isolated by mechanical fragmentation. The single-crystal intensity data were collected at r. t. using a Nonius Kappa-CCD diffractometer with graphite-monochromatized MoK_α radiation (λ = 71.073 pm). A semiempirical absorption correction based on equivalent and redundant intensities (SCALEPACK [26]) was applied to the intensity data. All relevant details of the data collection and evaluation are listed in Table 1. According to the systematic extinctions, the monoclinic space group $P2_1/c$ was derived. Because α-MnB_2O_4 is isotypic to α-FeB_2O_4 [15], the structural refinement was performed *via* the positional parameters of α-FeB_2O_4 as starting values (full-matrix least-squares on F^2; SHELXL-97 [27]). All atoms were refined with anisotropic displacement parameters, and the final difference Fourier syntheses did not reveal any significant peaks in the refinement. Tables 2 – 5 list the positional parameters, anisotropic displacement parameters, interatomic distances, and angles.

Further details of the crystal structure investigation may be obtained from Fachinformationszentrum Karlsruhe, 76344 Eggenstein-Leopoldshafen, Germany (fax: +49-7247-808-666; e-mail: crysdata@fiz-karlsruhe.de, http://www.fiz-

Table 3. Anisotropic displacement parameters of α-MnB_2O_4 (space group: $P2_1/c$) with standard deviations in parentheses.

Atom	U_{11}	U_{22}	U_{33}	U_{12}	U_{13}	U_{23}
Mn1	0.01019(10)	0.00889(10)	0.00838(9)	0.00121(6)	−0.00179(7)	0.00014(6)
Mn2	0.00763(9)	0.00921(10)	0.00841(9)	0.00026(6)	0.00018(7)	−0.00250(6)
B1	0.0063(5)	0.0062(5)	0.0057(5)	−0.0003(4)	0.0003(4)	−0.0003(4)
B2	0.0065(5)	0.0055(5)	0.0055(5)	0.0003(4)	0.0009(4)	0.0001(4)
B3	0.0068(5)	0.0048(5)	0.0055(5)	0.0001(4)	0.0011(4)	0.0001(4)
B4	0.0071(5)	0.0055(5)	0.0052(5)	0.0000(4)	0.0005(4)	0.0003(4)
O1	0.0094(4)	0.0047(4)	0.0058(3)	−0.0011(3)	−0.0001(3)	0.0000(3)
O2	0.0071(4)	0.0064(4)	0.0059(3)	0.0013(3)	0.0024(3)	0.0014(3)
O3	0.0052(3)	0.0075(4)	0.0072(3)	0.0003(3)	0.0013(3)	−0.0017(3)
O4	0.0047(3)	0.0073(4)	0.0100(4)	−0.0002(3)	0.0013(3)	−0.0019(3)
O5	0.0070(4)	0.0054(4)	0.0080(4)	−0.0009(3)	−0.0003(3)	0.0012(3)
O6	0.0072(4)	0.0078(4)	0.0053(3)	−0.0022(3)	0.0009(3)	0.0010(3)
O7	0.0094(4)	0.0054(4)	0.0060(3)	0.0011(3)	−0.0011(3)	−0.0011(3)
O8	0.0099(4)	0.0071(4)	0.0047(3)	0.0024(3)	0.0005(3)	−0.0006(3)

Table 4. Interatomic distances (pm) in α-MnB_2O_4 (space group: $P2_1/c$) calculated with the single-crystal lattice parameters (standard deviations in parentheses).

Mn1–O5	210.9(2)	Mn2–O6	208.7(2)
Mn1–O1	218.0(2)	Mn2–O3	212.5(2)
Mn1–O4a	220.7(2)	Mn2–O8	221.0(2)
Mn1–O2	222.2(2)	Mn2–O7	225.4(2)
Mn1–O4b	237.0(2)	Mn2–O1	234.9(2)
Mn1–O7	257.5(2)	Mn2–O2	240.8(2)
Mn1–O8	267.7(2)	Mn2–O3	252.2(2)
av.	233.4	av.	227.9
B1–O3	146.9(2)	B2–O1	146.3(2)
B1–O6	147.6(2)	B2–O7	147.2(2)
B1–O5	148.0(2)	B2–O2	148.9(2)
B1–O2	149.3(2)	B2–O3	150.0(2)
av.	148.0	av.	148.1
B3–O8	145.7(2)	B4–O5	146.3(2)
B3–O6	147.2(2)	B4–O8	147.1(2)
B3–O4	148.3(2)	B4–O7	148.9(2)
B3–O1	149.1(2)	B4–O4	150.0(2)
av.	147.6	av.	148.1

Table 5. Interatomic angles (deg) in α-MnB_2O_4 (space group: $P2_1/c$) calculated with the single-crystal lattice parameters (standard deviations in parentheses).

O3–B1–O6	105.7(2)	O1–B2–O7	110.8(2)
O3–B1–O5	108.2(2)	O1–B2–O2	112.2(2)
O6–B1–O5	113.9(2)	O7–B1–O2	109.9(2)
O3–B1–O2	112.5(2)	O1–B2–O3	104.0(2)
O6–B1–O2	109.8(2)	O7–B2–O3	113.2(2)
O5–B1–O2	106.8(2)	O2–B2–O3	106.6(2)
av.	109.5	av.	109.5
O8–B3–O6	111.3(2)	O5–B4–O8	114.4(2)
O8–B3–O4	114.2(2)	O5–B4–O7	110.2(2)
O6–B3–O4	104.6(2)	O8–B4–O7	109.4(2)
O8–B3–O1	110.9(2)	O5–B4–O4	108.7(2)
O6–B3–O1	108.9(2)	O8–B4–O4	108.3(2)
O4–B3–O1	106.6(2)	O7–B4–O4	105.6(2)
av.	109.4	av.	109.4

informationsdienste.de/en/DB/icsd/depot_anforderung.html) on quoting the deposition number CSD-423381.

Vibrational spectra

The confocal Raman spectra of single crystals in the range of 65 – 4000 cm^{-1} were achieved by a Horiba Jobin Yvon LabRam-HR 800 Raman micro-spectrometer. The samples were excited using the 532 nm emission line of a 100 mW Nd : YAG-laser and the 633 nm line of a 17 mW helium-neon laser. The size and power of the laser spot on the surface were approximately 1 μm and 2 – 5 mW, respectively. The spectral resolution was about 2 cm^{-1}, determined by measuring the Rayleigh line. The dispersed light was collected by a 1024×256 open electrode CCD detector. The spectra were recorded unpolarized. Background and Raman bands were fitted by the built-in spectrometer software LABSPEC to second order polynomial and convoluted Gaussian-Lorentzian functions, respectively. The accuracy of the Raman line shifts, calibrated by regularly measuring the Rayleigh line, was in the order of 0.5 cm^{-1}.

The FTIR-ATR (*A*ttenuated *T*otal *R*eflection) spectra of single crystals were recorded with a Bruker Vertex 70 FT-IR spectrometer (spectral resolution 4 cm^{-1}), equipped with a MCT (*m*ercury *c*admium *t*elluride) detector and attached to a Hyperion 3000 microscope in the spectral range of 600 – 4000 cm^{-1}. As mid-infrared source a *Globar* (silicon carbide rod) was used. A frustum-shaped germanium ATR-crystal with a tip diameter of 100 μm was pressed on the surface of the borate crystal with a power of 5 N, which crushed it into pieces of μm-size. 32 scans of the sample and the background were acquired. Beside the spectra correction for atmospheric influences, an enhanced ATR-correction [28], using the OPUS 6.5 software, was performed. A mean refraction index of the sample of 1.6 was assumed for the ATR-correction. Background correction and peak fitting were applied using polynomial and convoluted Gaussian-Lorentzian functions.

Results and Discussion

Crystal structure of α-MnB_2O_4

The structure of α-MnB_2O_4 is built up exclusively from distorted corner-sharing BO_4 tetrahedra

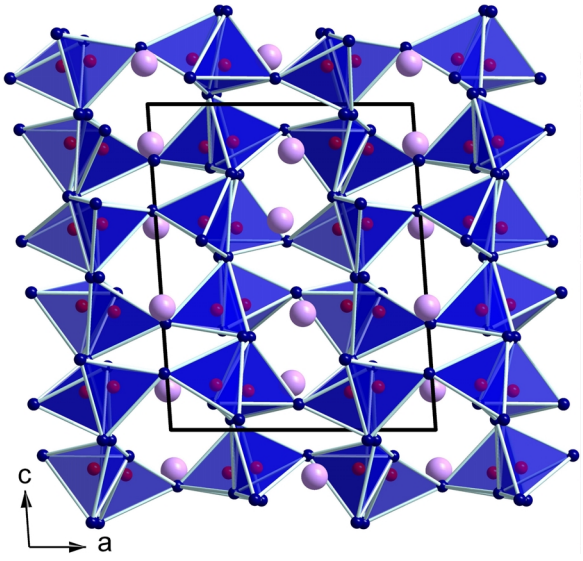

Fig. 1 (color online). Projection of the crystal structure of α-MnB_2O_4 along [010]. Polyhedra: BO_4 tetrahedra; large (rose) spheres: Mn^{2+}; corners of polyhedra (blue spheres): O^{2-}; center of polyhedra (red spheres): B^{3+}.

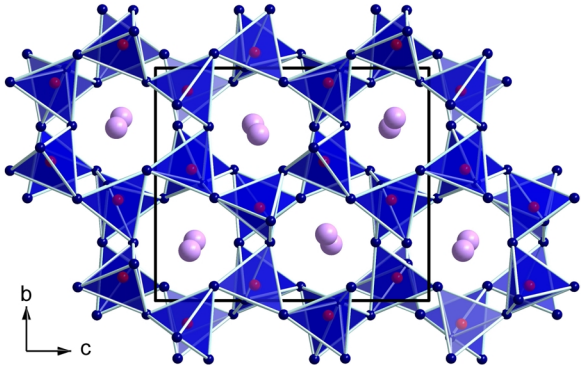

Fig. 2 (color online). Crystal structure of α-MnB_2O_4 with a view along [100], exhibiting layers of "sechser" rings of corner-sharing BO_4 tetrahedra. Polyhedra: BO_4 tetrahedra; large (rose) spheres: Mn^{2+}; corners of polyhedra (blue spheres): O^{2-}; center of polyhedra (red spheres): B^{3+}.

that form layers in the *bc* plane. Along [100], these layers are condensed to a three-dimensional network. Fig. 1 gives a view of the condensed borate layers along [010]. As depicted in Fig. 2, the layers consist of "sechser" rings [29] of BO_4 tetrahedra that form channels along [100], in which the manganese cations are situated. A closer look on the orientation of the BO_4 tetrahedra, building up one ring, reveals that there exists only one topology, namely DDUUDU (D = down, U = up). Fig. 3 shows this topology on a single layer of α-MnB_2O_4; light (yellow) BO_4 tetrahedra face downwards (D), dark (blue) BO_4 tetrahedra face upwards (U)).

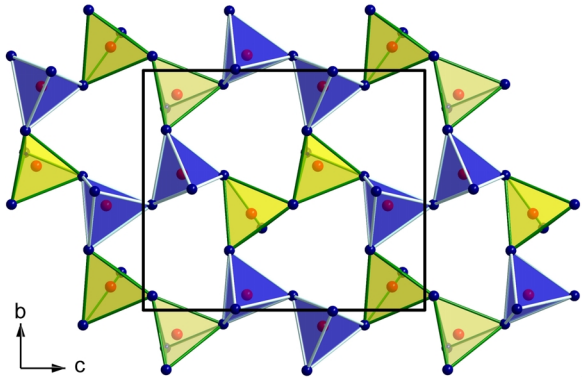

Fig. 3 (color online). Single layer of the B–O network of α-MnB_2O_4 viewed along [100]. The layer is built up from "sechser" rings with the topology DDUUDU [light (yellow) BO_4 tetrahedra face downwards (D), dark (blue) BO_4 tetrahedra face upwards (U)].

The high-pressure phase α-MnB_2O_4 is isotypic to α-FeB_2O_4 [15] and $CaAl_2O_4$-II [16], [17]], as well as to the normal pressure phases $CaGa_2O_4$ [18] and β-$SrGa_2O_4$ [19]. It shows the same topology as the orthorhombic compound $BaFe_2O_4$ [30], which exhibits a different connectivity of the layers, leading to a different crystal structure. Additionally, α-MnB_2O_4 is closely related to the high-pressure compound CdB_2O_4 [31]. The cadmium borate also consists of condensed layers of "sechser" rings of corner-sharing BO_4 tetrahedra, but with a different topology. However, all mentioned compounds can be understood as stuffed derivates of the tridymite framework structure.

In α-MnB_2O_4, the B–O bond lengths range between 145.7 and 150.0 pm with a mean value of 148.0 pm (Table 4). This value is slightly increased in comparison to the average distance of 147.6 pm in BO_4 tetrahedra [32, 33]. The O–B–O angles in the four different BO_4 tetrahedra vary from 104.0 to 114.4° and average out to 109.5° (Table 5). Fig. 4 shows that both crystallographically independent Mn^{2+} ions have a seven-fold coordination by the oxygen ions. The Mn–O distances vary between 208.7 and 267.7 pm and average out to 230.7 pm. This value is in good agreement with the average Mn^{2+}–O bond length of 228.3 pm for seven-fold coordinated Mn^{2+} in δ-Mn_2GeO_4 [34].

The bond valence sums of α-MnB_2O_4 were calculated for all atoms, using the CHARDI concept

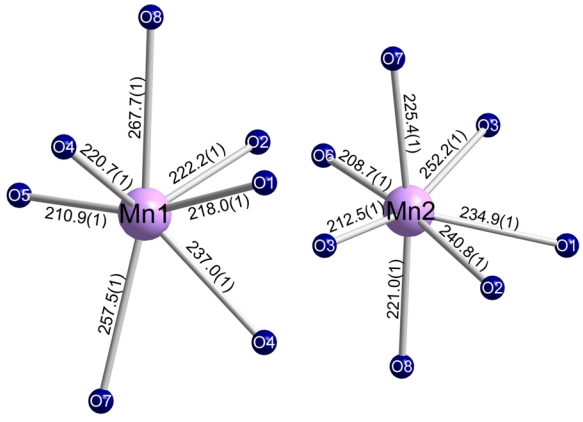

Fig. 4 (color online). Coordination spheres of the Mn^{2+} ions.

(*Charge distribution in solids*, ΣQ) [35] and the bond length/bond strength concept (ΣV) [36, 37]. The results of both concepts confirm the formal ionic charges, resulting from the crystal structure [ΣQ: +1.97 (Mn1), +2.02 (Mn2), +3.01 (B1), +3.01 (B2), +2.97 (B3), +3.03 (B4), −2.14 (O1), −1.97 (O2), −1.99 (O3), −2.03 (O4), −2.04 (O5), −1.98 (O6), −1.89 (O7), −1.97 (O8) and ΣV: +1.83 (Mn1), +2.01 (Mn2), +2.99 (B1), +2.98 (B2), +3.02 (B3), +2.98 (B4), −2.07 (O1), −1.95 (O2), −2.01 (O3), −1.98 (O4), −1.95 (O5), −1.96 (O6), −1.89 (O7), −1.88 (O8)].

Furthermore, the MAPLE values (*Madelung part of lattice energy*) [38–40] of α-MnB_2O_4 were calculated to compare them with the MAPLE values received from the summation of the binary components MnO [41] and the high-pressure modification B_2O_3-II. The value of 26348 kJ mol^{-1} was obtained in comparison to 26306 kJ mol^{-1} (deviation = 0.2 %), starting from the binary oxides (MnO (4368 kJ mol^{-1}) [41] + B_2O_3-II (21938 kJ mol^{-1}) [42]).

Despite their isotypy, there are rather large differences in the structures of α-MnB_2O_4 and α-FeB_2O_4. They result from the different ionic radii and the electronic configuration of the metal ions that are also influencing the boron oxygen network. Table 6 compares the different unit cells, the coordination numbers, the ionic radii [43, 44] of the metal ions, and the bond lengths. As expected, the unit cell volume rises with the increased ionic radius of Mn^{2+}. A closer look at the lattice parameters *a* and *b* (Table 5) reveals only a minor difference. In contrast, the lattice parameter *c* shows a remarkable difference of 16.5 pm. Thus, compared to α-FeB_2O_4, the *bc* layer of α-MnB_2O_4 is significantly expanded in the *c* direction. Interestingly, the length of the *a* axis, which is perpendicular to the condensed layers, even slightly decreases for α-MnB_2O_4. In α-MnB_2O_4, the *M*1 holds an increased coordination number (CN = 7) compared to α-FeB_2O_4, where it is only six-fold coordinated (the corresponding seventh oxygen ion in α-FeB_2O_4 has a distance of 301 pm). The increased coordination number in α-MnB_2O_4 is probably correlated with the larger ionic radius of Mn^{2+}, leading to a slight dislocation of Mn1 in the direction of O7 (see Fig. 5).

Table 6. Comparison of the isotypic structures α-MnB_2O_4 and α-FeB_2O_4 (both monoclinic $P2_1/c$).

Empirical formula	α-MnB_2O_4	α-FeB_2O_4
Molar mass, g mol^{-1}	140.6	141.5
Unit cell dimensions		
a, pm	712.1(2)	715.2(2)
b, pm	747.1(2)	744.5(2)
c, pm	878.8(2)	862.3(2)
β, deg	94.1(1)	94.7(1)
V, nm^3	0.4663(2)	0.4576(2)
Ionic radius for M^{2+} [52, 53]	1.04	0.99[a]
Coordination number (CN)		
*M*1 (*M* = Mn, Fe)	7	6
*M*2 (*M* = Mn, Fe)	7	7
av. *M*1–O (*M* = Mn, Fe) distance, pm	233.4	218.5
av. *M*2–O (*M* = Mn, Fe) distance, pm	227.9	225.0
av. B–O distance, pm	148.0	147.6

[a] Value is not given in refs. [52, 53] for CN = 7, but estimated from values for CN = 6 and CN = 8.

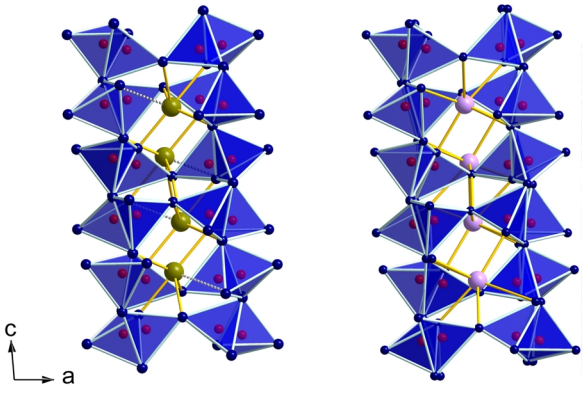

Fig. 5 (color online). Comparison of the relative *M*1 positions in α-FeB_2O_4 (left) and α-MnB_2O_4 (right). In α-MnB_2O_4, Mn1 is deflected into the direction of the seventh coordination partner.

Vibrational spectroscopy

Spectra of the Raman and FTIR-ATR measurements of α-MnB_2O_4 are displayed in Figs. 6 and 7, respectively. The assignments of the vibrational modes are based on a comparison with the experimental data

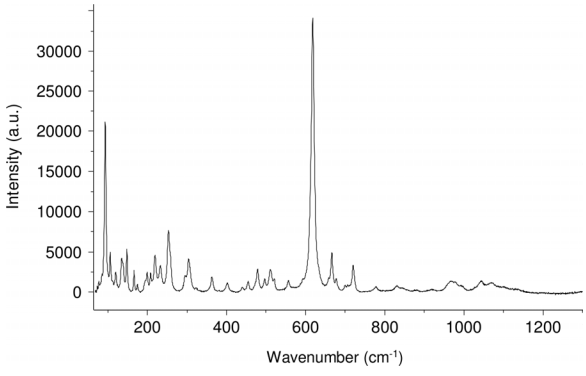

Fig. 6. Confocal Raman spectrum of an α-MnB_2O_4 single crystal in the range of 65 – 1300 cm^{-1}.

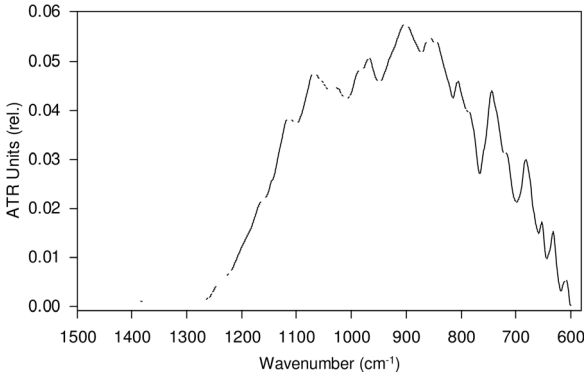

Fig. 7. ATR (*a*ttenuated *t*otal *r*eflection) spectrum of an α-MnB_2O_4 single crystal in the range of 1500 – 600 cm^{-1}.

of borate glasses and crystals, containing BO_3 and BO_4 building units [33, 45 – 49]. For borates in general, bands in the region of 800 – 1100 cm^{-1} usually apply to stretching modes of boron which is tetrahedrally coordinated to oxygen [50, 51]. Absorption and Raman bands at 1200 – 1450 cm^{-1} are expected for borates containing BO_3 groups, which do not occur in the structure of α-MnB_2O_4.

The Raman spectrum (Fig. 6) exhibits a dominant band at 615 cm^{-1}, weaker bands at 665 – 719 cm^{-1}, and weak bands at 832, 875, 962, 1043, and 1132 cm^{-1}. Bands below 800 cm^{-1} can be assigned to complex bending and stretching vibrations of the B–O network, Mn–O bonds, and lattice vibrations. In the range of 3000 to 3600 cm^{-1}, where vibrational modes caused by O–H stretching are expected, no bands could be detected.

In the FTIR spectrum, several groups of absorption bands were observed between 680 and 1135 cm^{-1}, the region where stretching modes of BO_4 tetrahedra occur. As for the Raman spectrum, no OH or water bands could be detected in the range of 3000 to 3600 cm^{-1}.

Conclusions

The monoclinic borate α-MnB_2O_4 is isotypic to α-FeB_2O_4, $CaAl_2O_4$-II, $CaGa_2O_4$, and β-$SrGa_2O_4$. It is built up from corner-sharing BO_4 tetrahedra that form a condensed layer structure. The layers consist of "sechser" rings of BO_4 tetrahedra that form channels along the *a* axis, in which the manganese cations are situated. For the orientation of the BO_4 tetrahedra building up one ring, there exists only one topology, namely DDUUDU (D = down, U = up).

Acknowledgements

We would like to thank Dr. G. Heymann for collecting the single-crystal data. Special thanks go to Univ.-Prof. Dr. R. Stalder for performing the IR measurements and to Univ.-Prof. Dr. V. Kahlenberg for providing the Raman micro-spectrometer.

[1] H. Huppertz, *Chem. Commun.* **2011**, *47*, 131.
[2] J. S. Knyrim, P. Becker, D. Johrendt, H. Huppertz, *Angew. Chem.* **2006**, *118*, 8419; *Angew. Chem. Int. Ed.* **2006**, *45*, 8239.
[3] S. C. Neumair, R. Glaum, H. Huppertz, *Z. Naturforsch.* **2009**, *64b*, 883.
[4] S. C. Neumair, R. Kaindl, H. Huppertz, *Z. Naturforsch.* **2010**, *65b*, 1311.
[5] J. S. Knyrim, F. Roeßner, S. Jakob, D. Johrendt, I. Kinski, R. Glaum, H. Huppertz, *Angew.Chem.* **2007**, *119*, 9256; *Angew. Chem. Int. Ed.* **2007**, *46*, 9097.
[6] S. C. Neumair, J. S. Knyrim, O. Oeckler, R. Glaum, R. Kaindl, R. Stalder, H. Huppertz, *Chem. Eur. J.* **2010**, *16*, 13659.
[7] J. S. Knyrim, J. Friedrichs, S. Neumair, F. Roeßner, Y. Floredo, S. Jakob, D. Johrendt, R. Glaum, H. Huppertz, *Solid State Sci.* **2008**, *10*, 168.
[8] S. C. Neumair, J. S. Knyrim, R. Glaum, H. Huppertz, *Z. Anorg. Allg. Chem.* **2009**, *635*, 2002.
[9] H. Huppertz, G. Heymann, *Solid State Sci.* **2003**, *5*, 281.
[10] S. C. Abrahams, J. L. Bernstein, P. Gibart, M. Robbins, R. C. Sherwood, *J. Chem. Phys.* **1974**, *60*, 1899.
[11] R. Sadanaga, T. Nishimura, T. Watanabe, *Mineral. J.* **1965**, *4*, 380.
[12] O. S. Bondareva, M. A. Simonov, N. V. Belov, *Kristallografiya* **1978**, *23*, 491.

[13] A. Utzolino, K. Bluhm, *Z. Naturforsch*. **1996**, *51b*, 1433.
[14] R. Norrestam, M. Kritikos, A. Sjödin, *J. Solid State Chem*. **1995**, *114*, 311.
[15] J. S. Knyrim, H. Huppertz, *J. Solid State Chem*. **2008**, *181*, 2092.
[16] S. Ito, K. Suzuki, M. Iagaki, S. Naka, *Mater. Res. Bull*. **1980**, *15*, 925.
[17] B. Lazic, V. Kahlenberg, J. Konzett, *Z. Kristallogr*. **2007**, *222*, 690.
[18] H. J. Deiseroth, H K. Müller-Buschbaum, *Z. Anorg. Allg. Chem*. **1973**, *402*, 201.
[19] V. Kahlenberg, R. X. Fischer, C. S. J. Shaw, *J. Solid State Chem*. **2000**, *153*, 294.
[20] N. Kawai, S. Endo, *Rev. Sci. Instrum.* **1970**, *8*, 1178.
[21] D. Walker, M. A. Carpenter, C. M. Hitch, *Am. Mineral.* **1990**, *75*, 1020.
[22] D. Walker, *Am. Mineral.* **1991**, *76*, 1092.
[23] D. C. Rubie, *Phase Transitions* **1999**, *68*, 431.
[24] H. Huppertz, *Z. Kristallogr.* **2004**, *219*, 330.
[25] J. W. Visser, *J. Appl. Crystallogr*. **1969**, *2*, 89.
[26] Z. Otwinowski, W. Minor in *Methods in Enzymology*, Vol. 276, *Macromolecular Crystallography*, Part A (Eds.: C. W. Carter Jr., R. M. Sweet), Academic Press, New York **1997**, p. 307.
[27] G. M. Sheldrick, SHELXS-97 and SHELXL-97, Programs for Crystal Structure Determination, University of Göttingen, Göttingen (Germany) **1997**. See also: G. M. Sheldrick, *Acta Crystallogr.* **1990**, *A46*, 467; *ibid.* **2008**, *A64*, 112.
[28] F. M. Mirabella, Jr., in *Internal Reflection Spectroscopy, Theory and Applications* (Ed.: F. M. Mirabella, Jr.), Marcel Dekker, New York **1993**, p. 17.
[29] The naming of rings of structural elements was coined by F. Liebau (*Structural Chemistry of Silicates*, Springer, Berlin **1985**) and is derived from German numbers, *e. g.* the term "sechser" ring is derived from the word "sechs", which means six. However, the term "sechser" ring does not mean a six-membered ring, but rather a ring with six tetrahedral centers (B) and six electronegative atoms (O).
[30] W. Leib, Hk. Müller-Buschbaum, *Z. Anorg. Allg. Chem*. **1986**, *538*, 71.
[31] J. S. Knyrim, H. Emme, M. Döblinger, O. Oeckler, M. Weil, H. Huppertz, *Chem. Eur. J*. **2008**, *19*, 6149.
[32] E. Zobetz, *Z. Kristallogr*. **1990**, *191*, 45.
[33] F. C. Hawthorne, P. C. Burns, J. D. Grice, *The Crystal Chemistry of Boron*, in *Boron: Mineralogy, Petrology and Geochemistry*, Mineralogical Society of America, Washington **1996**.
[34] N. Morimoto, M. Tokonami, K. Koto, S. Nakajima, *Am. Min.* **1972**, *57*, 62.
[35] R. Hoppe, S. Voigt, H. Glaum, J. Kissel, H. P. Müller, K. J. Bernet, *J. Less-Common Met.* **1989**, *156*, 105.
[36] I. D. Brown, D. Altermatt, *Acta Crystallogr.* **1985**, *B41*, 244.
[37] N. E. Brese, M. O'Keeffe, *Acta Crystallogr.* **1991**, *B47*, 192.
[38] R. Hoppe, *Angew. Chem.* **1966**, *78*, 52; *Angew. Chem., Int. Ed. Engl*. **1966**, *5*, 95.
[39] R. Hoppe, *Angew. Chem.* **1970**, *82*, 7; *Angew. Chem., Int. Ed. Engl*. **1970**, *9*, 25.
[40] R. Hübenthal, MAPLE (version 4), Program for the Calculation of Distances, Angles, Effective Coordination Numbers, Coordination Spheres, and Lattice Energies, University of Gießen, Gießen (Germany) **1993**.
[41] V. M. Goldschmidt, T. Barth, D. Holmsen, G. Lunde, W. Zachariasen, *Skr. Nor. Vidensk.-Akad., Mat.-Naturvidensk. Kl.* **1926**, *1*, 5.
[42] C. T. Prewitt, R. D. Shannon, *Acta Crystallogr.* **1968**, *B24*, 869.
[43] R. D. Shannon, C. T. Prewitt, *Acta Crystallogr.* **1969**, *B25*, 925.
[44] R. D. Shannon, *Acta Crystallogr.* **1976**, *A32*, 751.
[45] H. Huppertz, *J. Solid State Chem*. **2004**, *177*, 3700.
[46] G. Chadeyron, M. El-Ghozzi, R. Mahiou, A. Arbus, J. C. Cousseins, *J. Solid State Chem.* **1997**, *128*, 261.
[47] L. Jun, X. Shuping, G. Shiyang, *Spectrochim. Acta* **1995**, *A51*, 519.
[48] G. Padmaja, P. Kistaiah, *J. Phys. Chem.* **2009**, *113*, 2397.
[49] J. C. Zhang, Y. H. Wang, X. Guo, *J. Lumin.* **2007**, *122 – 123*, 980.
[50] M. Ren, J. H. Lin, Y. Dong, L. Q. Yang, M. Z. Su, L. P. You, *Chem. Mater*. **1999**, *11*, 1576.
[51] J. P. Laperches, P. Tarte, *Spectrochim. Acta* **1966**, *22*, 1201.
[52] R. D. Shannon, C. T. Prewitt, *Acta Crystallogr*. **1969**, *B25*, 925.
[53] R. D. Shannon, *Acta Crystallogr*. **1976**, *A32*, 751.